International Journal of Current Engineering and Technology
E-ISSN 2277 – 4106, P-ISSN 2347 – 5161

Available at http://inpressco.com/category/ijcet

Research Article

Influence of Hydrothermal Synthesis Reaction Duration on the Properties of Cu_2ZnSnS_4 (CZTS) Thin Films

Kasim Ibrahim Mohammed[1,4,*], Kasim Uthman Isah[1], Uno Esang Uno[1], Abdullahi Mann[2] and Nafarizal Nayan[3]

[1]Department of Physics, Federal University of Technology, Minna, Nigeria
[2]Department of Chemistry, Federal University of Technology, Minna, Nigeria
[3]Microelectronics and Nanotechnology Shamsuddin Research Centre (MiNT-SRC), Institute for Integrated Engineering (I²E), Universiti Tun Hussein Onn Malaysia, 86400 Parit Raja, Johor, Malaysia
[4]Department of Physical Sciences, Niger State Polytechnic, Zungeru, Nigeria

Received 15 July 2019, Accepted 16 Sept 2019, Available online 26 Sept 2019, **Vol.9, No.5 (Sept/Oct 2019)**

Abstract

Cu_2ZnSnS_4 (CZTS) films were synthesised using hydrothermal method, while varying the reaction duration from 12 h to 48 h in steps of 12 h. The XRD reveal characteristic peaks of CZTS (112) and (220) for the samples 150_24, 150_36 and 150_48 and in addition (200) and (312) peaks for samples 150_36 and 150_48. The average crystallite sizes range between 18.00 and 19.00 nm. Raman spectra of the films reveal CZTS peaks of 338, 351 and 252 cm^{-1}, in addition to secondary and ternary phases observed for samples other than 24 h. SEM image show spherical nanoparticles and agglomerated nanosphere-like shapes. The Cu: Zn: Sn: S atom ratios were close to stoichiometry at 24 h and 36 h hydrothermal synthesis duration. There is significant deviation from stoichiometry at other durations. The average surface roughness was between 800 and 2000 nm. The bandgap energy obtained from the optical characterisation varied between 1.52 eV and 1.51 eV.

Keywords: *Cu_2ZnSnS_4, Hydrothermal, Reaction Duration, Thin film, Nanoparticles*

1. Introduction

Cu2ZnSnS4 (CZTS) is one of the most promising absorber layer materials for low-cost thin film solar cells due to its semiconductor properties such as p-type conductivity, direct band gap and high absorption coefficient (≥10^4 cm^{-1}), as well as the earth abundant and nontoxic constituent elements (T. Ahmet *et al*, 2018). This semiconductor film can be regarded as an alternative to ($CuInSe_2$) CIS and ($CuInGaSe_2$) CIGS materials, in which the extremely expensive and resource limited Indium is replaced by cheap and abundant zinc (Zn) and tin (Sn). CZTS films have been synthesised and deposited by several vacuum and non-vacuum methods such as physical vapour deposition methods like atom beam sputtering, evaporation, sputtering and sequential evaporation, co-evaporation, multi-stage evaporation and pulsed laser deposition. Also chemical deposition methods like photo-chemical deposition, sol gel, spray pyrolysis, vapour-phase sulphurisation of E-B evaporated precursors and hydrothermal have been used (U. Chalapathi *et al*, 2015). The non-vacuum based methods especially the solution chemical method offers handy, simple, compact equipment's, low wastage of raw materials with low capital investment. A solution synthesis hydrothermal method for the CZTS thin films is based on the synthesis of nanocrystals. The nanocrystals allows band tuning which facilitates multiple electron-hole pair generations per incident photon and promises opportunities for use in high-efficiency photovoltaic devices (S. Das et al, 2018). Well controlled stoichiometry is an advantage of solution synthesis route for nanocrystals for use in CZTS based thin film solar cells. The nanocrystals can be easily converted into thin films by either doctor blading or spin coating of the nanocrystals slurry from the hydrothermal reaction (M. Fernandes *et al*, 2009).

Among various non-vacuum based solution synthesis routes, the hydrothermal route is one of the well-known and efficient methods since it is low cost and environmentally friendly. The hydrothermal route can be used to synthesise free standing nanostructures with various morphologies. Moreover, the hydrothermally synthesized CZTS nanocrystals have better crystallinity as compared to other methods. Literatures have shown that variation in reaction duration also plays a vital role in the structure of the thin film materials obtained using hydrothermal synthesis (T. Tiong *et al*, 2014).

*Corresponding author's ORCID ID: 0000000221646981
DOI: https://doi.org/10.14741/ijcet/v.9.5.6

In this work we report CZTS thin film preparation by doctor blading of hydrothermally synthesised nanoparticles on FTO doped soda lime glass substrate while varying the reaction duration. By this inexpensive process the CZTS absorber layer can be prepared easily, which may be useful for solar cell application.

Methodology

All the chemicals used were purchased from Sigma Aldrich unless otherwise stated. 0.2 mmol of $CuCl_2.2H_2O$, 0.1 mmol of $ZnCl_2$, 0.1 mmol of $SnCl_4.5H_2O$, 0.5 mmol of C_2H_5NS and 1.0 g of (PAA) were dissolved in 36 ml of water under magnetic stirring. The resulting solution was transferred to a Teflon-lined stainless steel autoclave of 45 ml capacity, which was then sealed and maintained at 150 °C for 12 h, 24 h, 36h and 48 h. After that, the autoclave in each case was allowed to cool to room temperature naturally.

The resulting black precipitate of each sample was centrifuged and washed with deionised water, absolute ethanol and acetone several times. Finally, the products were vacuum-dried at 80 °C for 5 hours. The samples were labelled 150_12, 150_24, 150_36 and 150_48 for samples synthesised at the hydrothermal reaction duration of 12 h, 24 h, 36 h and 48 h respectively.

The dried powders obtained from as-synthesized CZTS nanocrystals were prepared for thin film deposition by dispersing the CZTS powder (10%, w/w) in mixture of terpineol and triton X-100 (85%:5%, w/w). The slurry was then subjected to rigorous magnetic stirring for 48 hours.

Thin films were then prepared by depositing the CZTS slurry on fluorine doped tin oxide (FTO) coated soda lime glass (FTO/SLG) substrate by doctor-blading. The thin films were then annealed in a graphite box containing sulphur powder at 550 °C for 30 min in a rapid thermal annealing processing (RTP) system with a heating rate of 10 °C/min. A static annealing atmosphere of 0.3 atm argon was supplied in the RTP furnace.

Before deposition, the substrate was prewashed thoroughly with deionised water, acetone, and ethanol in sequence under sonication for 10 min each followed by being blow-dried with nitrogen gas.

The crystallographic structure and phase analysis of the synthesized thin film samples were done by X-ray diffraction (XRD, PANanalytical XPert Pro Multi-Purpose Diffractometer (MPD), CuKα, λ = 0.154056 nm). The Raman spectra of the samples were recorded with a Raman spectrometer (Xplora Plus, Horiba Scientific Raman microscope) with a 785 nm excitation laser to distinguish possible secondary phases in the films. The morphology and the elemental analysis of the samples were characterised by scanning electron microscopy (SEM, JEOL 7600F) at an acceleration voltage of 20.0 kV combined with an energy dispersive X-ray spectroscopy (EDS). Surface roughness and topology measured using (Hitachi 5100N) atomic force microscope (AFM). Ultraviolet-visible (UV-vis) absorption spectrum of the samples was measured at room temperature using a Shimadzu UV-1800 spectrophotometer. The Infra-red spectra of the samples were measured using Perkin-Elmer, G-FTIR spectrometer. The thickness of the films was measured using Alpha step Q 7083319 surface profiler, while the electrical resistivity measurement of the thin film samples was done using (signatone PRO 4, LUCAS LABS 2400) four point probe.

Results and Discussion

Figure 1 below show the XRD patterns of the CZTS thin film samples obtained at different reaction durations.

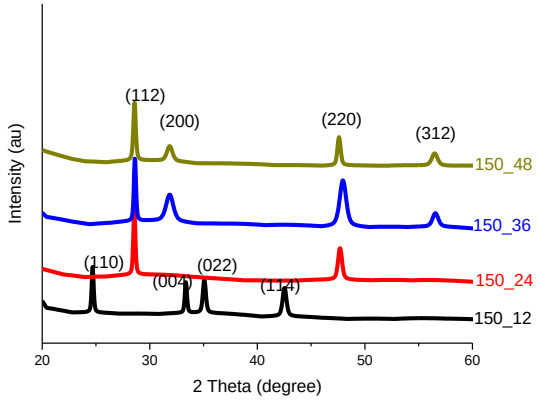

Figure 1: XRD patterns for CZTS thin film samples synthesised at different reaction durations

Variation in reaction duration also plays a vital role in the structure of the thin film material. The peaks at 2θ values of 28.60°, 31.83°, 47.69° and 56.39° correspond to CZTS *h k l* parameters (*112*), (*200*), (*220*) and (*312*) respectively for samples 150_48 and 150_36. The peaks (110), (004), (022) and (114) identified for sample 150_12 reveal that only $Cu_{2-x}S$, SnS_2 , ZnS and Cu_2SnS_3 were formed, suggesting that each metal ions in the precursor solution firstly reacted with Thioacetamide to form binary and ternary sulphides. This is in agreement with the results in the literatures (T. Tiong *et al*, 2014). When the reaction proceeded for 24 hours, CZTS compound was formed as confirmed by the (112) and (220) peaks which are for CZTS compounds. This implies that CZTS was actually formed through the reaction between the binary sulphide ZnS and ternary sulphide in the hydrothermal reaction. All the XRD diffraction peaks in samples 150_24, 150_36 and 150_48 can be well indexed to the corresponding crystal planes of kesterite CZTS (JCPDS 01-75-4122). From the XRD pattern, all films in the three samples show preferential orientation along (112) plane having the most prominent peak. The peaks at 2θ values of 28.59°, 47.70°, 33.04 and 57.54 correspond to lattice planes (112), (220), (200) and (312) respectively of kesterite CZTS (ICSD 98-018-4358). At 24 h, only (112) and (220) peaks were observed but at longer hydrothermal reaction duration

of 36 h and 48 h, the peaks (200) and (312) were observed in addition to the (112) and (220) this is also in agreement with literature reports [9]. The peak of CZTS at 2θ value of 28.59° is observed to shift left by 0.26 degrees in 150_36 sample. This shift might be due to changes in d-spacing values of the corresponding plane. Using the most prominent peaks in each sample, the crystallite sizes of the samples were calculated using Debye Scherer's formula as shown in table 1.0 below;

$$D = \frac{\kappa\lambda}{\beta\cos\theta} = \frac{0.94\lambda}{\beta\cos\theta}$$

Where β is full width at half maximum (FWHM), θ is diffraction angle, k is a constant of approximate 0.94 Shape factor and λ is wavelength of the X-rays (1.5406 Å or 0.15406 nm) and D is crystallite size respectively.

Table 1.0: FWHM and Crystallite size of CZTS thin films for reaction duration variation

Sample name	FMHW (°)	Crystallite size (nm)	2θ (°)	d-spacing (Å)	Hkl	Lattice parameters a(Å)
150_12	14.28	18.75	24.99	2.94716	110	5.41
150_24	14.30	19.00	28.59	3.12209	112	5.41
150_36	14.30	18.50	28.57	2.95420	112	5.43
150_48	14.28	18.00	28.60	3.12095	112	5.43

Crystallite size of the films increased with rise in reaction duration from 12 hours to 24 hours. After 24 hour reaction duration, the crystallite size decreased. The lattice parameter 'a' were close to the value of 5.4270 Å for tetragonal unit cell kesterite CZTS. The crystal interplanar spacing of 3.12 Å, can be ascribed to the (112) plane of kesterite phase CZTS. The crystallite sizes range between 18.00 and 19.00 nm, the 150_24 sample had the highest crystallite size and the 150_48 sample had the least size of 18.00 nm.

Definitive structural analysis and electronic excitation states of the lattice that provide information on possible secondary phases in a material is provided by Raman Spectroscopy. Raman scattering gives a more definitive structure analysis (K. Ito, 2015). The Raman spectra are shown in figure 2.0 below.

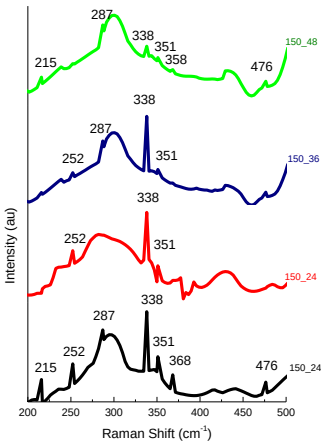

Figure 2.0 Raman spectra for CZTS samples synthesised at different reaction durations

The Raman spectra clearly show the peaks 338 cm^{-1}, 351 cm^{-1}, 252 cm^{-1}, 287 cm^{-1} and 351 cm^{-1} which are CZTS peaks (K. Nagoya *et al*., 2010). At durations higher than 24 hours (that is at 36 and 48 hours) the 215 cm^{-1} and 476 cm^{-1} peaks appeared. The 215 cm^{-1} peak in the literatures is usually associated with SnS_2 and 476 cm^{-1} usually associated with $Cu_{2-x}S$ (K. Nagoya *et al*., 2010). The 215 cm^{-1} and 476 cm^{-1} peaks which are secondary phases also appeared in the sample reacted for 12 hours. It can also be observed that at duration of 48 hours, the main CZTS 338 cm^{-1} peak was weakened indicating decomposition of the compound. The $Cu_{2-x}S$, and SnS_2 binary secondary phases observed at 12 hours duration suggests that the Cu and Sn metal ions in the precursor solution have started reacting with thioacetamide to form the CZTS compound.

The SEM images of the synthesised samples shown below in figure 3.0 below illustrates that the thin films were composed of several intersectional spherical shaped particle. When the hydrothermal reaction proceeded for 12 h, the sample was dominated by uniform and well-dispersed spherical flower-like particles. Homogenous sphere-like particles were formed at 24 h of reaction time. The agglomeration of flower-like particles was observed at 36 h duration. The particles further aggregated to form large agglomeration at 48 h of reaction duration indicating the further reactions forming impurities.

The particle size as determined using image J app also increase when the reaction duration was increased from 12 h to 24 h and then decreased as the duration was increase from 24 h to 48 h. 15 nm for sample 150_12, 17 nm for 150_24, 16 nm for 150_36 and 16 nm for 150_48. These values are very close to those observed in the XRD. The EDS data shows that the film composed of Cu, Zn, Sn and S as shown in Table 2.0 below.

From table 2.0 below, the atomic percentage of Cu and S did not show significant changes as reaction duration increases from 12 h to 48 h. The ideal CZTS stoichiometric ratio entails Cu/(Zn + Sn) and Zn/Sn be equals 1, while the ideal the ideal Cu: Zn: Sn: S stoichiometric value is 2:1:1:4. The 150_24 and 150_36 samples reveal near ideal compositional ratio for Cu/Zn + Sn of 0.91 and 0.84, Zn/Sn ratio of 0.87 and 0.75 respectively, these values though shows they are both Cu poor and Zn poor. Cu/(Zn + Sn) atomic ratio of near 0.85 have however been reported to show good optoelectronic properties and best device efficiency.

The slightly Sn rich and Zn poor composition for 150_24 and 150_36 may be ascribed to the reactivities of the different metal precursor (A. Wei *et al*, 2015). The Cu:Zn:Sn:S ratios of 1.97:1.00:1.35:4.17 and 2.04:1.00:1.34:4.09 for the 150_24 and 150_36 samples respectively were close to ideal stoichiometric value of 2:1:1:4. Samples 150_12 and 150_48 however show significant deviation from ideal CZTS composition exhibiting very high Sn content. These samples show significant decrease in the Zn/Sn ratio. The Zn/Sn ratios shows the samples are Sn rich and Zn poor.

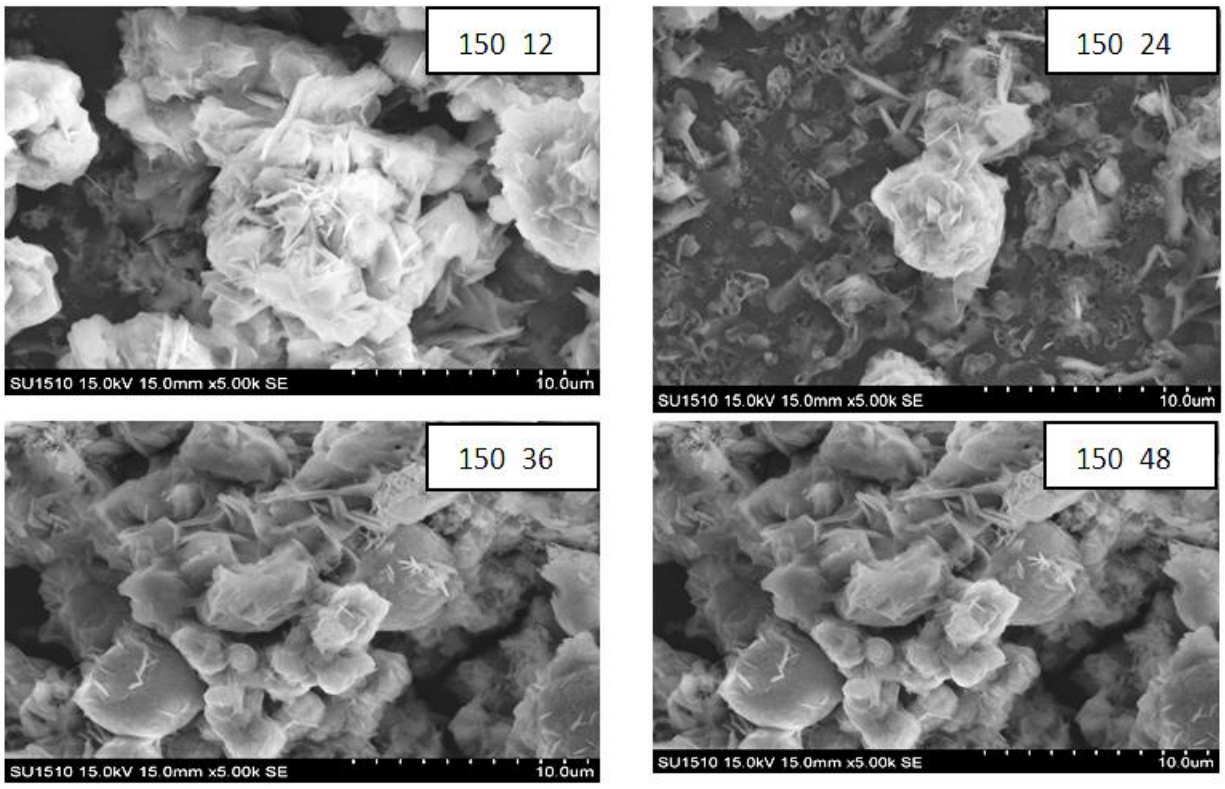

Figure 3.0: SEM images for CZTS samples synthesised at different reaction duration

Table 2.0: EDS Data for CZTS Thin Film Samples at Different Duration

Sample	Cu (at.%)	Zn (at.%)	Sn (at.%)	S (at.%)	$\frac{Cu}{Zn+Sn}$	$\frac{Zn}{Sn}$	Cu/Zn/Sn/S
150_12	22.4	6.1	17.7	48.6	0.94	0.34	3.67:1.00:2.90:7.79
150_24	23.1	11.8	13.5	48.9	0.91	0.87	1.97:1.00:1.35:4.17
150_36	22.7	11.6	15.5	47.4	0.84	0.75	2.04:1.00:1.34:4.09
150_48	22.3	7.6	19.7	48.0	0.82	0.39	2.93:1.00:2.59:6.32

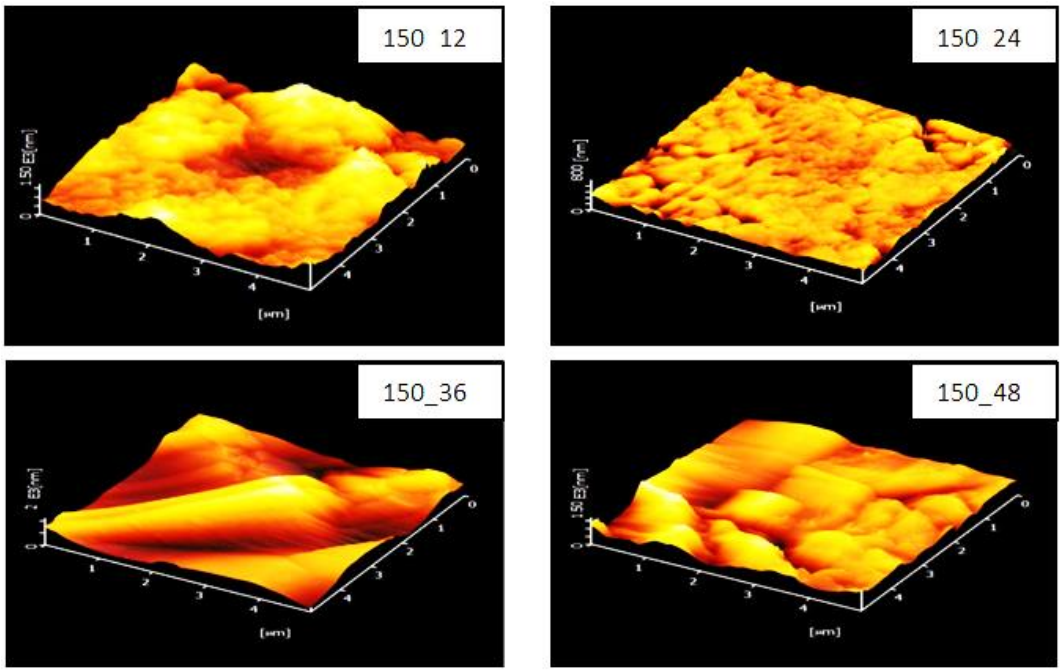

Figure 4.0 AFM images for the CZTS samples synthesised at different reaction durations

Figures 4.0 above show the AFM images of CZTS thin film samples synthesised at different hydrothermal reaction temperatures. AFM provides 3-Dimensional and 2-Dimensional profiles of the sample surface on a nanoscale. In this work, it is observed from the figure that the morphology of these films was uniform surface with clear grain boundaries and growth of crystal. A small decrease in surface roughness from 12 h to 24 h was observed and then surface roughness increased from 24 h to 36 h and then decreased again from 36 h to 24 h. The average surface roughnesses of the materials are shown in table 3.0 below.

High Surface roughness values affect device performance and may even lead to pinholes which are detrimental as they cause shunting in thin film device fabrication. From the results, all the values obtained are in good agreement with literature values (S. Das *et al*, 2018). But for the best performing device, lower value surface roughness (that is 0.8 x 10^3 nm for sample 150_24) is most appropriate.

For a direct band gap material the absorption coefficient satisfy the relation:

$$(\alpha h\nu)^2 = A(h\nu - Eg)$$

where α, ν, Eg and A are the absorption coefficient, light frequency, band gap energy and a constant respectively. The direct band gap Eg calculated by extrapolating the linear portion of the curves of $(\alpha h\nu)^2$ vs. (hν) gives values of Eg as shown in table 3.0 and figure 5.0 below. The bandgap and also the absorption coefficient values are in good agreement with the reported values in literature (U. Chalapathi *et al*, 2015). These values are close to optimal bandgap and absorption coefficient of 1.45 eV and 10^4 cm^{-1} respectively for absorber layer application in solar cells.

Table 3.0 Band gap, absorption coefficient, surface roughness and electrical resistivity of CZTS material at different temperatures

S/N	Sample	Absorption coefficient (A) (cm^{-1})	Band gap (Eg) (eV)	Surface Roughness (nm)	Resistivity (Ωcm)
1	150_12	1.31 X 10^4	1.52	1.5 x 10^3	4.40 x 10^{-2}
2	150_24	1.37 X 10^4	1.51	0.8 x 10^3	4.03 x 10^{-2}
3	150_36	0.87 X 10^4	1.51	2.0 x 10^3	2.63 x 10^{-2}
4	150_48	0.89 X 10^4	1.52	2.0 x 10^3	1.00 x 10^{-2}

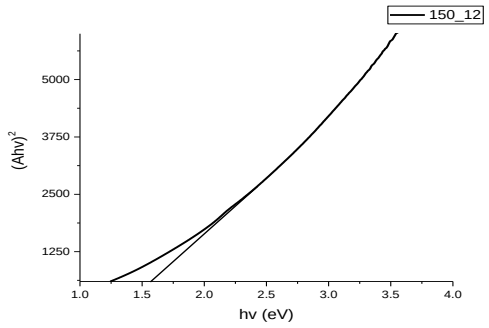

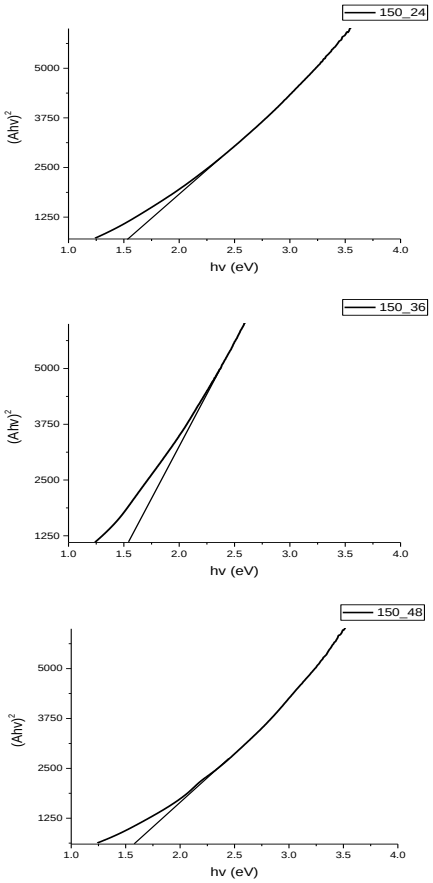

Figure 5.0: Energy band gap analyses for CZTS thin film samples synthesised at different reaction durations

As complementary characterizations, the FTIR analysis was carried out for the samples. FTIR response for the four samples is shown in figure 6.0 below. It reveals the presence of various bands at 630, 1129 and 1451cm^{-1}. In addition to the usual signature of water observed in samples 150_36 and 150_12 (K. Ito 2015), peaks observed at 1129cm^{-1} is usually attributed to metal–sulphur complexes. Bands around 900–1600cm^{-1} are due to oxygen stretching and banding frequency. Weak additional bands at 950 and 884cm^{-1} are attributed to the resonance interaction between vibrational modes of sulphide ions in the crystal.

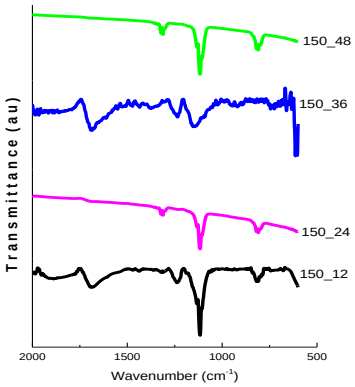

Figure 6.0: FTIR spectra for CZTS thin film samples synthesised at different reaction durations

The thickness of thin films have critical role in the properties of thin films. In this present work, it is observed that irrespective of the variation in hydrothermal reaction duration, the film thickness was approximately 3.6 x 10^{-1}µm.

Resistivity values decrease with increase in hydrothermal reaction duration from 12 h to 24 h. All the resistivity values obtained exhibited the p-type semiconductor material property of 10^{-2} Ωm as shown in Table 3.0 above.

Conclusion

This research work systematically examined the effects of various reaction durations on the formation of CZTS nanocrystals using the hydrothermal method. Kesterite CZTS were obtained at duration of 24 h with no secondary phase, secondary and ternary phases were observed at 12 h, 36 h and 24 h. The Cu:Zn:Sn:S ratios of 1.97:1.00:1.35:4.17 and 2.04:1.00:1.34:4.09 for the 150_24 and 150_36 samples respectively were close to ideal stoichiometric, there is however significant stoichiometric deviation for the samples 150_12 and 150_24, exhibiting significant Zn deficiency. The optical band gap of the sample samples was between 1.51 and 1.52 eV.

For pure phase CZTS material that has the capacity for being used as best solar cell absorber material, the hydrothermal reaction conditions should be 150 ^{0}C for 24 hours reaction duration. It was revealed that the reaction duration used in the hydrothermal reaction process influences both the compositional and stoichiometry of the crystal structure of the synthesised samples.

References

Ahmet, T., Abdullah, G., Muharram, Z. Z. & Ferhat, A. (2018), Structure, morphology and optical properties of the vacuum-free processed CZTS thin film absorbers. *Materials Research Express,* (59), pp 102-104.

Chalapathi, U., Uthanna, S. & Raja, S. (2015), Growth of Cu_2ZnSnS_4 thin films by a two stage process-Effect of incorporating of sulfur at the precursor stage, *Solar Energy Materials and Solar Cells,* (132), pp 476-484

Das, S., Sa, K., Mahakul, P. C., Raiguru, J., Alam, I., Subramanyam, B. V. R. S and Mahanandia, P (2018), Synthesis of quaternary chalcogenide CZTS nanoparticles by a hydrothermal route, *IOP Conf. Series, Materials Science and Engineering* (338), pp 12-15

Fernandes, M., Cao, L., Zhang, B. L. & Jiang, J. C. (2009), One step deposition of CZTS thin films for solar cells, *Solar Energy Materials and Solar Cells*, (117), pp 81-86

Ito, K. (2015), *Copper Zinc Tin Sulfide-Based thin film solar cells*, John Wiley and Sons Ltd. Pp 93-199

Katagiri H., Jimbo K., Maw W. S., Oishi K., Yamazaki M., Araki H., *et al*. (2009), Development of CZTS-based thin film solar cells, *Thin Solid Films* (517), pp 2455-2460

Nagoya, K. V., Pawara, S. M., Shinb, S. W., Moona, J. H. & Kima, P. S. (2010), Electrosynthesis of CZTS films by sulfurization of CZT precursor: effect of soft annealing treatment, *Applied Surface Science*, (238), pp 74-80

Price, D. B., Mitzi, O., Gunawan, T. k. & Wang, K. (1999), The path towards a high performance solution-processed kesterite CZTS, *Solar Energy Materials and Solar Cells,* (95), pp 1421-1436

Tiong, T. T., Hreid, T., Will, G., Bell, J., & Wang, H. (2014), Polyacrylic acid assisted synthesis of CU_2ZnSnS_4 by hydrothermal method, *Science of Advanced Materials*, (6), pp 1467-1474

Wadia, C., Alivisatos, A. P. & Kammen, D. (2009), CZTS-based solar cell from sol-gel spin coating and its characterization, *Evironment Science and Technology,* (43), pp 2072-2077

Wang, K., Mitzi, D. B., Barkhouse, R. & Aaron, D. (2011), Prospects and performance limitations for Cu-Zn-Sn-S-Se photovoltaic technology, *Philadelvia Transnational Royal Society,* (371), pp 1-22

Wei A., Yan, Z., Zhao, Y., Zhuang, M. and Liu, J. (2015), Solvothermal synthesis of Cu_2ZnSnS_4 nanocrystalline thin films for application of solar cells, *International Journal of Hydrogen Energy*, (40), pp 797-805